Inorganic Chemistry

ARTICLE

pubs.acs.org/IC

Near-Infrared Absorbing and Emitting Ru^{II}—Pt^{II} Heterodimetallic Complexes of Dpdpz (Dpdpz = 2,3-Di(2-pyridyl)-5,6-diphenylpyrazine)

Si-Hai Wu,[†] Stephen E. Burkhardt,[‡] Jiannian Yao,[†] Yu-Wu Zhong,*[,†] and Héctor D. Abruña*[,‡]

[†]Beijing National Laboratory for Molecular Sciences, CAS Key Laboratory of Photochemistry, Institute of Chemistry, Chinese Academy of Sciences, Beijing 100190, P. R. China

[‡]Baker Laboratory, Department of Chemistry and Chemical Biology, Cornell University, Ithaca, New York 14853-1301, United States

Supporting Information

ABSTRACT:

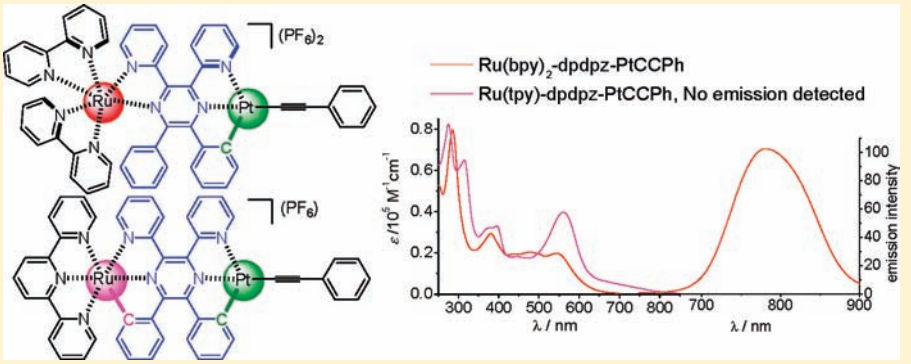

The reaction of 2,3-di(2-pyridyl)-5,6-diphenylpyrazine (dpdpz) with K_2PtCl_4 in a mixture of acetonitrile and water afforded mono-Pt complex (dpdpz)$PtCl_2$ **4** in good yield, with two lateral pyridine nitrogen atoms binding to the metal center. Two types of Ru^{II}—Pt^{II} heterodimetallic complexes bridged by dpdpz, namely, $[(bpy)_2Ru(dpdpz)Pt(C{\equiv}CC_6H_4R)]^{2+}$ (**7**—**9**, R = H, NMe_2, or Cl, respectively) and $[(tpy)Ru(dpdpz)Pt(C{\equiv}CPh)]^{+}$ (**12**), were then designed and prepared, where bpy = 2,2′-bipyridine and tpy = 2,2′;6′,2″-terpyridine. In both cases, the platinum atom binds to dpdpz with a C^N^N tridentate mode. However, the coordination of the ruthenium atom with dpdpz could either be noncyclometalated (N^N bidentate) or cyclometalated (C^N^N tridentate). The electronic properties of these complexes were subsequently studied and compared by spectroscopic and electrochemical analyses and theoretical calculations. These complexes exhibit substantial absorption in the visible to NIR (near-infrared) region because of mixed MLCT (metal-to-ligand-charge-tranfer) transitions from both the ruthenium and the platinum centers. Complexes **7** and **9** were found to emit NIR light with higher quantum yields than those of the mono-Ru complex $[(bpy)_2Ru(dpdpz)]^{2+}$ (**5**) and bis-Ru complex $[(bpy)_2Ru(dpdpz)Ru(bpy)_2]^{4+}$ (**13**). However, no emission was detected from complex **8** or **12** at room temperature in acetonitrile.

INTRODUCTION

Materials that can absorb and emit light in the near-infrared (NIR) region (700—1000 nm) are the subject of intensive research.[1] NIR dyes are particularly interesting for biological imaging, because NIR light exhibits low light scattering and deep penetration behaviors. More importantly, most biological samples absorb weakly in the long-wavelength region, thus decreasing the background absorbance and autofluorescence. Besides, NIR dyes have been studied in other applications such as solar cell,[2] optoelelctronic devices,[3] and chemosensors and probes.[4] Representative NIR emitting materials include some cyanines dyes, rhodamine derivatives, phthalocyanines, boron-dipyrromethene (BODIPY) dyes,[5] quantum dots,[6] and extended aromatic carbon materials.[7] However, some of these materials suffer from low emission quantum yields, short lifetime, and lack of photostability and biocompatibility. Hence, new NIR emitting dyes with superb optical properties are still in demand.

One of the promising alternatives is polynuclear transition metal complexes. Complexation of transition-metals with organic ligands provides molecular structures with rigid and well-defined geometries. Optimal orbital overlap between metals and ligands delocalize electrons along the entire molecule, which consequently narrows its highest occupied molecular orbital (HOMO) to lowest unoccupied molecular orbital (LUMO) gap, and absorbs visible/NIR light intensively.[8] Because of their

Received: November 28, 2010
Published: March 29, 2011

Scheme 1. Synthesis of $Ru^{II}-Pt^{II}$ Heterodimetallic Complexes of dpdpz

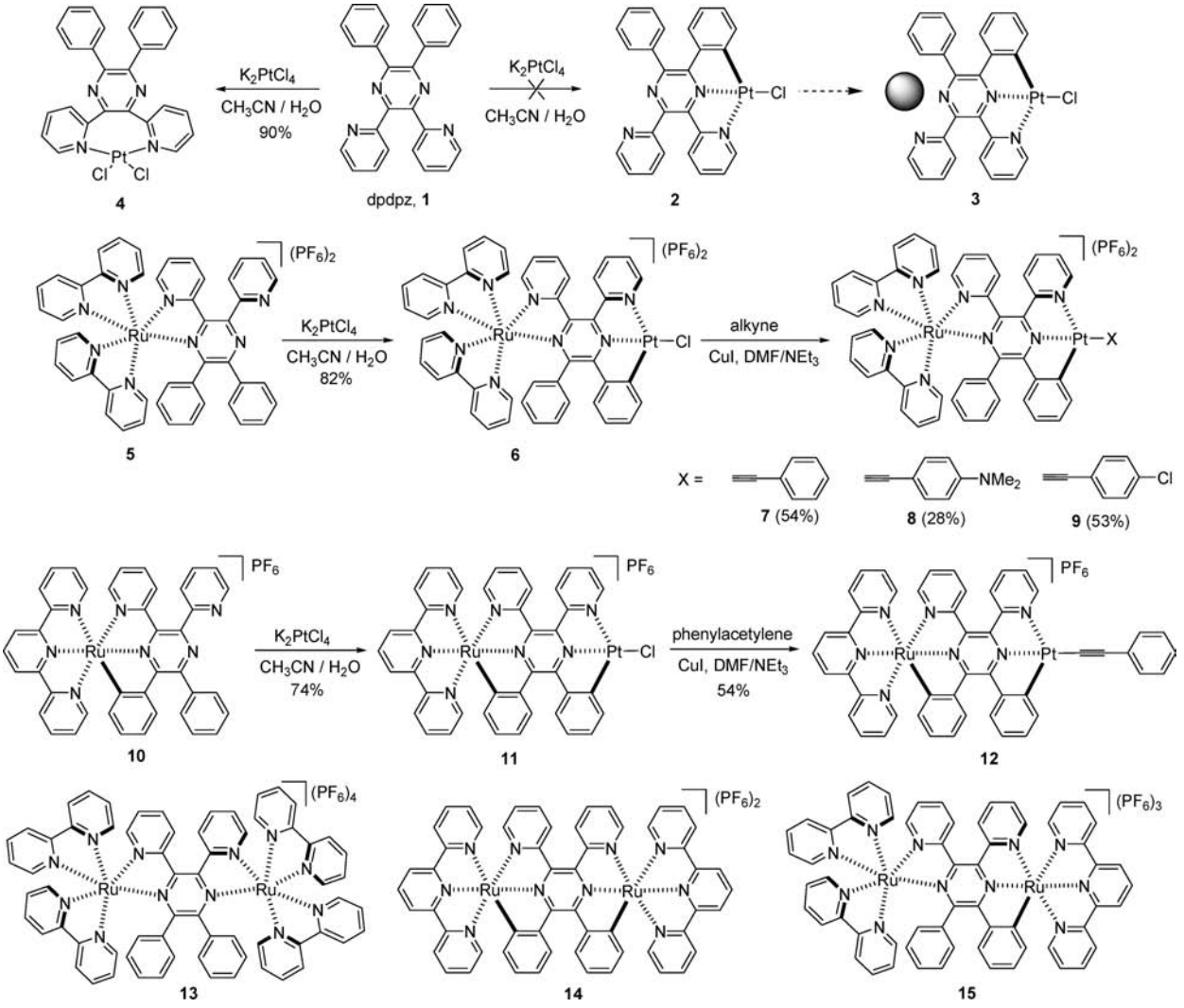

appealing electrochemical and photophysical properties, transition-metal polyazine complexes have been extensively employed for this purpose.[9] A simple and general way to construct polymetallic coordination oligomers or polymers is to assemble metal centers using appropriate bridging ligands, such as 2,3,5,6-tetrakis(2-pyridyl)pyrazine (tppz)[10] and 2,3-bis(2-pyridyl)pyrazine (dpp).[11] These ligands have been used to construct a large number of rigid molecular architectures when bound to transition-metal ions such as Ru^{II}, Os^{II}, Re^{I}, Cu^{I}, and Pt^{II}. Some of the complexes prepared in this way absorb visible light strongly because of the metal-to-the-ligand-charge-transfer transition (MLCT) and give rise to triplet Vis/NIR emission at room temperature with a relatively long lifetime. These complexes have been widely used as light harvesting or emitting materials in optoelectronic devices and many photoinduced energy/electron transfer processes.

Cyclometalated polyazine complexes[12] have been the recent subject of intensive research activities, particularly those containing iridium(III),[13] Pt(II),[14] and Ru(II)[15] metal centers. The anionic nature of the ancillary ligand significantly changes the properties of cyclometalated complexes, as compared to non-cyclometalated ones. For example, the $Ru^{II/III}$ redox process of $[Ru(tpy)_2]^{2+}$ (tpy = 2,2′;6′,2″-terpyridine) occurs at +1.32 V vs Ag/AgCl, meanwhile the ruthenium center of a related cyclometalated complex, $[Ru(tpy)(dpb)]^{+}$ (dpb = 1,3-di(2-pyridyl)-benzene), can be oxidized at much less positive potential (+0.53 V vs Ag/AgCl).[15] Square planar complex $[Pt(tpy)Cl]^{+}$ is virtually nonemissive at room temperature, meanwhile related cyclometalated platinum complexes, either $[Pt(dpb)]Cl$[16] or $[Pt(pbp)]Cl$[17] (pbp = 6-phenyl-2,2′-bipyridine), give substantial emission.

We previously reported a bridging ligand dpdpz **1** (dpdpz = 2,3-di(2-pyridyl)-5,6-diphenylpyrazine, Scheme 1), and its complexation with ruthenium atoms.[18] This ligand was designed so that it could bridge two metal species with either a N^N-type bidentate or a C^N^N tridentate coordination mode. The key is whether or not the two lateral phenyl rings in dpdpz are involved in the coordination with metal species. If the phenyl rings are connected to a metal center, dpdpz is expected to behave as a C^N^N-type tridentate ligand to form cyclometalated complexes. However, if phenyl rings remain intact, dpdpz could behave as a N^N-type bidentate binding ligand. In this way, we have prepared two symmetric and one asymmetric diruthenium complexes, with each ruthenium being cyclometalated or non-cyclometalated. The electrochemical and photophysical properties

dx.doi.org/10.1021/ic1023696 |*Inorg. Chem.* 2011, 50, 3959–3969

of these complexes are found to greatly depend on the coordination mode of metals. For example, cyclometalated ruthenium complexes have rigid linear conformation, narrower energy gaps, and lower redox potentials of the metal centers. Noncyclometalated complexes were found to emit at room temperature. We envisage that cyclometalating ligand dpdpz **1** could also be used to prepare a square planar Pt^{II} complex, such as complex **2** shown in Scheme 1. The other half of the ligand then could bind to various metal centers, either in a N^N-type bidentate or a C^N^N tridentate coordination mode, to give rise to a variety of M-Pt heterodimetallic systems **3**. This kind of complex would be expected to emit NIR light because of the electron delocalization across the whole molecule. However, as will be described in the following section, we failed to isolate the platinum complex **2** at this stage. Instead, we successfully prepared heterodimetallic Ru−Pt complexes **6**−**9**, **11**, and **12** starting from the monometallic ruthenium complex **5** or **10**. Complexes **7** and **9** were found to emit NIR light at room temperature, with even a higher quantum yield than monoruthenium complex **5**. We report herein the syntheses and characterization of these complexes. The spectroscopic, electrochemical, and theoretical calculation studies of these complexes are also presented and compared with previously reported diruthenium complexes **13**−**15**.

RESULTS AND DISCUSSION

Synthesis. The syntheses of dpdpz **1** and complexes **5** and **10** have been described in a previous paper.[18] As for the preparation of cyclometalated Pt^{II} complexes, two reaction media are routinely employed in the literature, namely acetic acid[19] or a mixture of acetonitrile and water.[20] Contrary to our expectation, the reaction of **1** with K_2PtCl_4 in a mixture of acetonitrile and water gave the mononuclear Pt^{II} complex **4**, with two lateral pyridine nitrogen atoms binding to the metal center, instead of the cyclometalated complex **2** (Scheme 1). It should be noted that Pt^{II} diimine complexes with similar 7-membered chelate rings have been reported in the literature.[21] Considering the electron-withdrawing character of the pyrazine moiety and wide binding angle of the two pyridine groups to the metal center, this complex may be suitable for catalyzing some organic transformations.[22] When the reaction was carried out in acetic acid, an unidentified solid was isolated, which has low solubility in most organic solvents, and we are unable to determine its structure at this stage.

The structure of the Pt^{II} complex **4** was determined by single crystal X-ray analysis (Figure 1), which confirmed that two pyridine nitrogen atoms bind to the Pt center in a bidendate α fashion.[23] The crystallographic data and selected bond lengths and angles are given in Tables 1 and 2. The binding angle of the two pyridine nitrogen atoms to the Pt atom, N(2)−Pt(1)−N(1), is 87.23°. In most Pt^{II}-2,2′-bipyridine complexes,[24] this angle is around 77−79°. Another intriguing structural feature of **4** is that the pyrazine ring is almost perpendicular to the plane defined by the platinum and two chlorine atoms (bottom in Figure 1). Work is underway to assemble this unusual structure into three-dimensional coordination systems.

The failure to obtain the cyclometalated platinum complex **2** from dpdpz **1** prompted us to investigate the reaction of K_2PtCl_4 with mono-Ru^{II} complex **5**, which has been reported previously.[18] Given that one of the pyridine groups in **5** has already been locked by coordination to a Ru atom, it would be easier to access the $[(C^N^N)Pt]^+$ moiety. This reaction took place smoothly, in a mixture of acetonitrile and water, to afford the crude heterodinuclear Ru^{II}−Pt^{II} complex **6** in good yield (82%, Scheme 1). However, simple reprecipitation or recrystallization could not give analytically pure sample. Attempts to

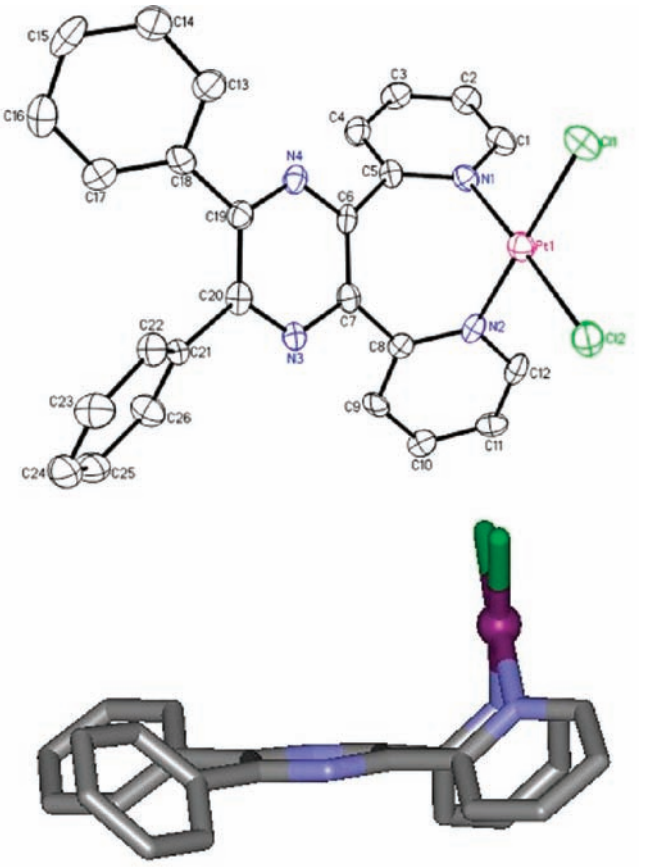

Figure 1. ORTEP drawing (up) and stick model (below) of complex **4**.

Table 1. Crystallographic Data Collection and Structure Refinement Parameters for the Pt^{II} Complex 4

	4
empirical formula	$C_{26}H_{18}Cl_2N_4Pt$
formula weight	652.43
space group	$P\bar{1}$
crystal system	triclinic
a (Å)	9.293(3)
b (Å)	10.736(3)
c (Å)	11.436(4)
α (deg)	85.311(14)
β (deg)	83.961(13)
γ (deg)	79.865(14)
vol ($Å^3$)	1114.6(6)
Z	2
temp (K)	173(2)
density (calcd)	1.944 mg/m^3
wavelength (Å)	0.71073
abs coeff (mm^{-1})	6.557
final R indices	R1 = 0.0345, wR2 = 0.0712
R indices (all data)	R1 = 0.0496, wR2 = 0.0745

dx.doi.org/10.1021/ic1023696 |*Inorg. Chem.* 2011, 50, 3959–3969

purify this product through flash column chromatography led to decomposition, likely because of the substitution of the chloride atom by solvent. Thus, we decided to prepare a derivative of this compound which could be fully characterized. In this sense, the reaction of **6** with phenylacetylene in the presence of CuI and triethylamine[25] gives the platinum acetylide complex **7** in 54% yield. In addition, complexes **8** and **9** with an electron-donating NMe_2 or electron-withdrawing Cl substituent were obtained to investigate the influence of substituents on their properties. We previously found that cyclometalated or noncyclometalated ruthenium complexes of dpdpz exhibited significantly different electrochemical and photophysical properties depending on the nature of the ruthenium atoms.[18] Thus, starting from the known cyclometalated mono-Ru^{II} complex **10**,[18] the heterodinuclear dicyclometalated $Ru^{II}-Pt^{II}$ complex **12** was also prepared in the same way for a comparison study.

Table 2. Selected Bond Lengths (Å) and Angles (deg) for the Pt^{II} Complex 4

Pt(1)−N(2)	1.988(4)	N(2)−Pt(1)−Cl(2)	89.57(1)
Pt(1)−N(1)	2.012(4)	N(1)−Pt(1)−Cl(2)	176.8(1)
Pt(1)−Cl(1)	2.2762(1)	Cl(1)−Pt(1)−Cl(2)	92.16(5)
Pt(1)−Cl(2)	2.2837(2)	C(1)−N(1)−Pt(1)	120.7(3)
N(2)−Pt(1)−N(1)	87.23(2)	C(5)−N(1)−Pt(1)	119.6(3)
N(2)−Pt(1)−Cl(1)	177.16(1)	C(12)−N(2)−Pt(1)	118.4(3)
N(1)−Pt(1)−Cl(1)	91.03(1)	C(8)−N(2)−Pt(1)	123.1(3)

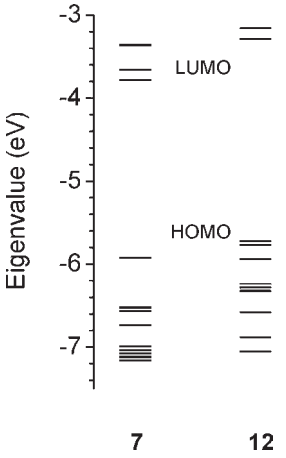

Figure 2. Frontier orbital energy level alignment of complexes **7** and **12**.

DFT Calculations. Density functional theory (DFT) calculations were performed on complexes **7** and **12** on the B3LYP/LANL2DZ level to assist the determination of their electronic structures. The frontier orbital energy level alignment of **7** and **12** is presented in Figure 2. The LUMO and HOMO of **7** reside at −3.76 and −5.91 eV, respectively. In comparison, both LUMO (−3.27 eV) and HOMO (−5.66 eV) of **12** are destabilized relative to those of **7**. Some frontier orbital structures of **7** and **12** with electron density distributions are shown in Figures 3 and 4, respectively. It is clear that both HOMOs of the two complexes are dominated by the platinum acetylide component, and both LUMOs have major contribution from the bridging dpdpz ligand. In lower occupied orbitals, the ruthenium center and the cyclometalated phenyl ring of dpdpz play an important role, such as HOMO-2, HOMO-3, and HOMO-5 of complex **7**, and HOMO-1 and HOMO-2 of complex **12**. In higher unoccupied orbitals, the ancillary bpy or tpy ligand contributes dominantly, such as LUMO + 2 of complex **7** and LUMO + 2 and LUMO + 3 of complex **12**.

Electrochemical Studies. Electrochemical studies were carried out on the above-prepared complexes to probe their electronic properties. The cyclic voltammograms (CV) profiles are shown in Figure 5 and Figures S1 and S2 in the Supporting Information, and their electrochemical data are summarized in Table 3, together with some related complexes for comparison. Noncyclometalated mono-Ru complex **5** displays one ruthenium-related reversible oxidation wave at +1.38 V vs Ag/AgCl (enrty 1 in Table 3).[18] In addition, one dpdpz-based reduction wave at −0.97 V and two bpy-based reduction waves at −1.40 and −1.73 V are evident in the CV profile of complex **5**.[18] When a cyclometalated platinum acetylide moiety is bound to the open coordination site of **5** to give complex **7**, the oxidation of Ru^{II} was found to occur at a more positive potential (+1.58 V vs Ag/AgCl, Figure 5a). The irreversible wave at +1.37 V could be ascribed to

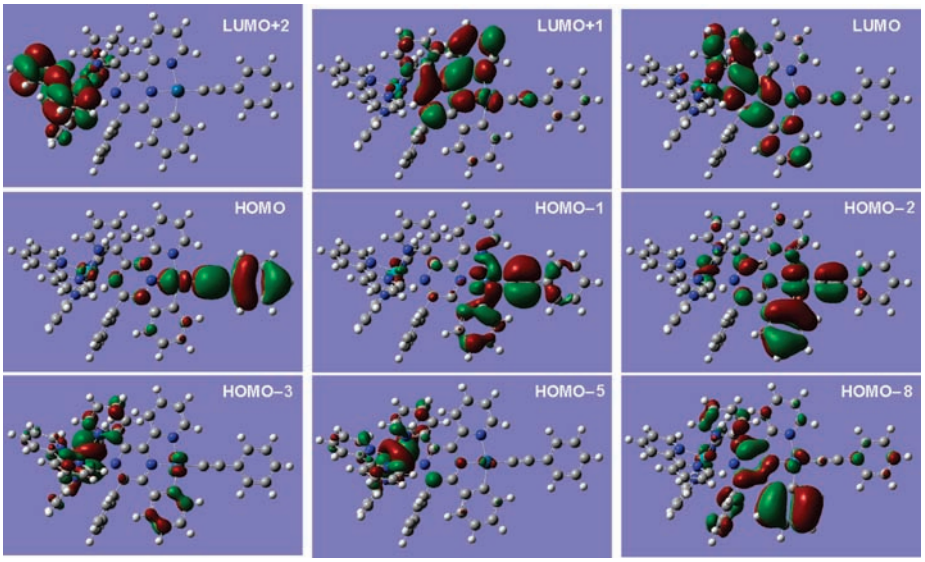

Figure 3. Isodensity plots of a few calculated HOMO and LUMO orbitals for complex **7**. All orbitals have been computed at an isovalue of 0.02.

dx.doi.org/10.1021/ic1023696 |*Inorg. Chem.* 2011, 50, 3959–3969

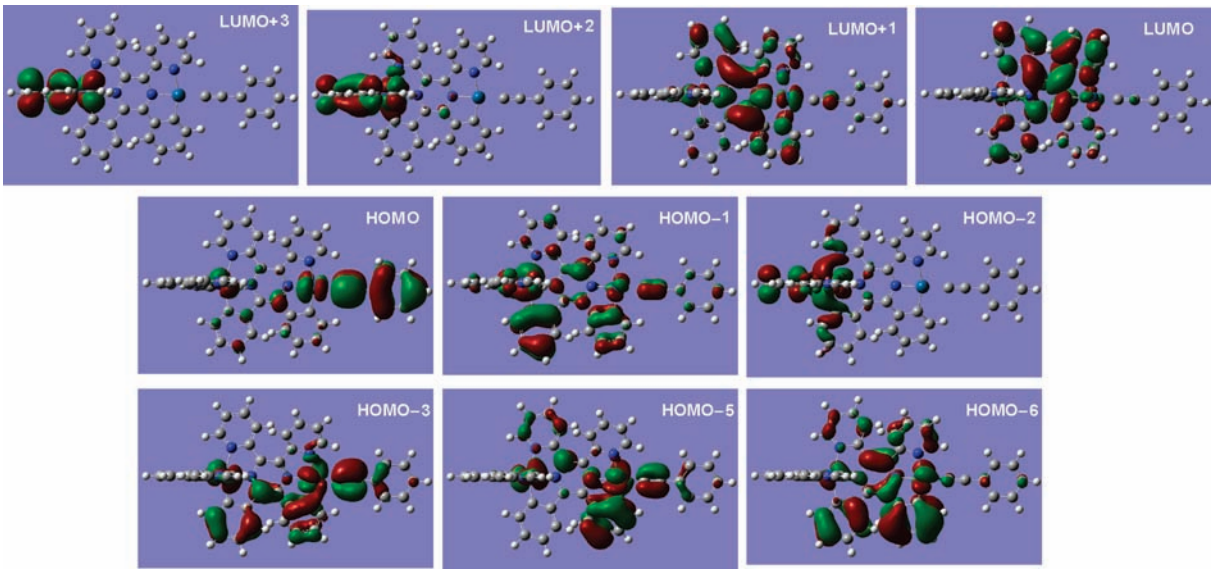

Figure 4. Isodensity plots of a few calculated HOMO and LUMO orbitals for complex **12**. All orbitals have been computed at an isovalue of 0.02.

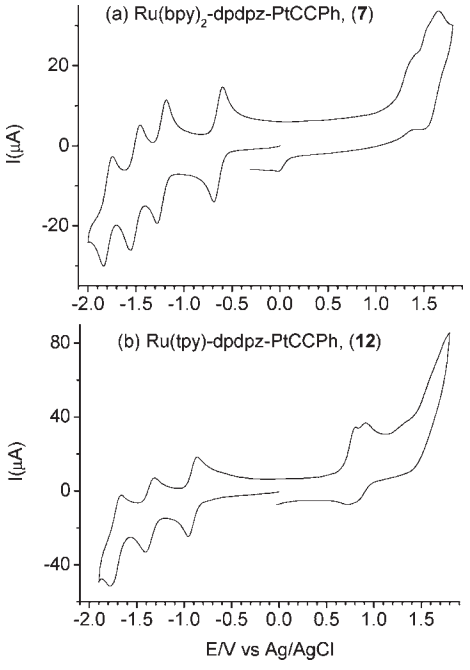

Figure 5. Cyclic voltammograms of complexes (a) **7** and (b) **12** in acetonitrile containing 0.1 M Bu_4NClO_4 at a scan rate of 100 mV/s. The working electrode is a glassy carbon, the counter electrode is a Pt wire, and the reference electrode is Ag/AgCl in saturated aq. NaCl.

the oxidation of the platinum center or platinum atcetylide component. The cathodic scan of **7** shows four redox couples at −0.65, −1.23, −1.51, and −1.79 V, respectively. The former two waves are attributable to the consecutive reductions of dpdpz, and the latter two waves are assigned to the reduction of bpy ligands. The assignments of these redox processes are in consistent with the above-described DFT calculations which predict that the platinum acetylide could be first oxidized and the bridging dpdpz ligand could be first reduced. On the basis of the electrochemical studies, it is clear that the addition of the cyclometalated platinum moiety to mono-Ru complex **5** leads to a significant positive-shift of the first dpdpz-based reduction process (−0.65 vs −0.97 V). This effect is stronger than the case when a cyclometalated Ru(tpy) moiety is bound to complex **5**, in which the first reduction of dpdpz was found to take place at −0.82 V (entry 3).[18] The electrochemical behaviors of complexes **8** and **9** (entries 4 and 5, Supporting Information, Figures S1 and S2, respectively) are closely similar to that of **7**, except in the case of the NMe_2-containing complex **8**, an additional irreversible wave at +0.57 V vs Ag/AgCl was found. This peak is assigned to the irreversible oxidation of the nitrogen atom.

The anodic scan of the cyclometalateed mono-Ru complex **10** displays two redox couples at +0.67 and +1.31 V vs Ag/AgCl (entry 6).[18] The former peak is assigned to the $Ru^{II/III}$ redox processes, and the latter one could either be attributed to $Ru^{III/IV}$ couple or ligand-based oxidative decomposition.[15] The cathodic scan of **10** shows one dpdpz-based reduction at −1.33 V and one tpy-based reduction at −1.71 V vs Ag/AgCl. In comparison, the biscyclometalated heterdinuclear Ru^{II}−Pt^{II} complex **12** exhibits three cathodic waves at −0.91, −1.37, and −1.72 V vs Ag/AgCl, respectively (Figure 5b and entry 7 in Table 3). The former two peaks are assigned to dpdpz reductions, and the peak at −1.72 V is attributable to the reduction of the ancillary tpy ligand. Again, the first dpdpz-based reduction of **12** occurs at a much less negative potential than those of mono-Ru complex **10** and biscyclometalated bis-Ru complex **14** (−0.91 vs −1.33 and −1.03 V, respectively). The anodic scan of **12** shows two redox couples at +0.77 and +0.87 V. According to the DFT calculations, HOMO of **12** is dominated by the platinum acetylide component and HOMO-1 is dominated by the cyclometalated ruthenium moiety. Thus, we tentatively assign the peak at +0.77 V to the oxidation of the platinum acetylide component, and the peak at +0.87 V to the $Ru^{II/III}$ process. From the comparison of the CV profiles of **7** and **12**, it is evident that the first cathodic wave of **12** occurs at a more negative potential than that of **7**, and the first anodic wave of **12** takes place at a less positive than that of **7**. This suggests that both the LUMO and the HOMO of **12** reside in a higher energy level than those of **7**, which is supported by DFT calculations as well.

dx.doi.org/10.1021/ic1023696 |*Inorg. Chem.* 2011, 50, 3959–3969

Table 3. Electrochemical Data of Complexes Studied[a]

			$E_{1/2}$ (ligand-based reduction)	
entry	complex	$E_{1/2}$ (anodic)	dpdpz	bpy or tpy
1	**5**, $[(bpy)_2Ru(dpdpz)](PF_6)_2$	1.38	−0.97	−1.40, −1.73
2	**7**, $[(bpy)_2Ru(dpdpz)PtC{\equiv}CPh](PF_6)_2$	1.37, 1.58	−0.65, −1.23	−1.51, −1.79
3	**15**, $[(bpy)_2Ru(dpdpz)Ru(tpy)](PF_6)_3$	0.81, 1.32, 1.57	−0.82, −1.25	−1.55, −1.73, −1.90
4	**8**, $[(bpy)_2Ru(dpdpz)PtC{\equiv}CC_6H_4NMe_2](PF_6)_2$	0.57, 1.27, 1.58	−0.66, −1.23	−1.50, −1.79
5	**9**, $[(bpy)_2Ru(dpdpz)PtC{\equiv}CC_6H_4Cl](PF_6)_2$	1.33, 1.58	−0.63, −1.24	−1.50, −1.79
6	**10**, $[(tpy)Ru(dpdpz)](PF_6)$	0.67, 1.31	−1.33	−1.71
7	**12**, $[(tpy)Ru(dpdpz)PtC{\equiv}CPh](PF_6)$	0.77, 0.87	−0.91, −1.37	−1.72
8	**14**, $[(tpy)Ru(dpdpz)Ru(tpy)](PF_6)_2$	0.65, 0.84, 1.33, 1.60	−1.03, −1.43	−1.73, −1.86

[a] All measurements were carried out in acetonitrile containing 0.1 M Bu_4NClO_4 as the supporting electrolyte. Unless otherwise noted, the potential is reported as the $E_{1/2}$ value vs Ag/AgCl.

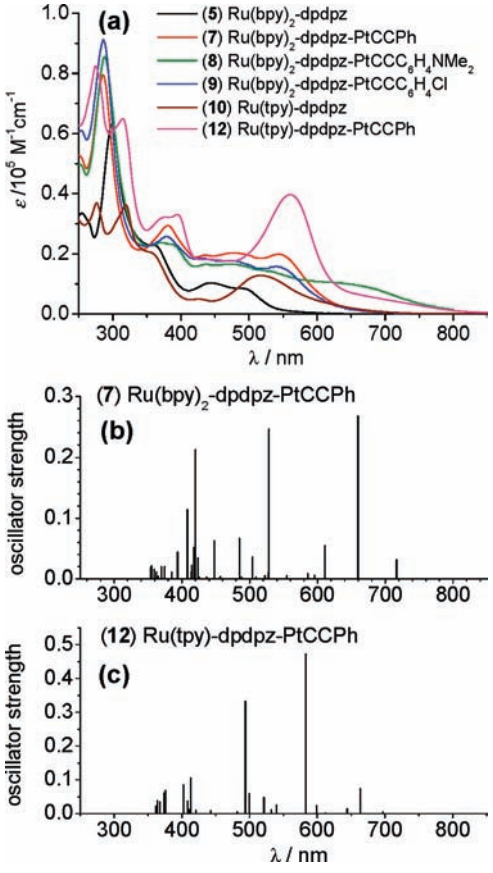

Figure 6. (a): UV/vis absorption spectra of complexes **5**, **7**−**10**, and **12** in acetonitrile. (b) and (c): first 40 absorptions as predicted by TDDFT for complex **7** and **12**, respectively.

Spectroscopic Studies and TDDFT Calculations. The electronic absorption spectra of the aforementioned complexes are shown in Figure 6a, and their absorption maxima and absorptivities are collected in Table 4. The UV region of the absorption spectra are dominated by intraligand $\pi-\pi^*$ excitations. The intense and broad bands in the visible region are mostly ascribed to MLCT transitions from both Ru and Pt components. To aid in the assignment of the optical absorptions more precisely, the nature of the low energy transitions was studied by time-dependent DFT (TDDFT) calculations. The first 40 predicted transitions of complex **7** and **12** are shown in Figure 6b and 6c, respectively. Tables 5 and 6 give major predicted transitions with the excitation energy, oscillator strength, dominant configuration contribution and assignment. The platinum-based MLCT transitions of C^N^N-type platinum acetylide complexes were reported to exhibit two absorption maxima at 440 and 460 nm,[14,26] which are at a similar energy level with the ruthenium-based MLCT transitions of $[Ru(bpy)_3]^{2+}$ (420 and 455 nm). On the basis of this fact, we could not assign the lowest energy MLCT band of complex **7** (545 nm). However, according to TDDFT results (S_1-S_3 in Table 5), this peak is dominated by an admixture of M_{Pt}LCT and LLCT (acetylide ligand to the bridging dpdpz ligand charge transition). The peak at 477 nm is an admixture of ILCT (intraligand charge transition from the cyclometalated phenyl ring of dpdpz to the azine-containing rings of the same ligand) and MLCT from both metal centers. The higher energy peak at 436 nm is assigned to M_{Ru}LCT.

The absorption spectrum of complex **9** is very similar to that of complex **7**. However, the introduction of a dimethylamino group on complex **8** leads to the emergence of a new low-energy band between 600−700 nm. This band is attributed to the $\pi[C{\equiv}CC_6H_4NMe_2] \rightarrow \pi^*[dpdpz]$ LLCT transition.[27] By comparison, biscyclometalated complex **12** displays an intense lowest energy band at 561 nm, with the low energy side extending over 800 nm. As suggested by TDDFT calculations, this peak is attributed to an admixture of M_{Pt}LCT/LLCT/M_{Ru}LCT, with mixed contributions of HOMO → LUMO, HOMO-1 → LUMO, HOMO → LUMO+1, HOMO-1 → LUMO+1 origins.

The emission properties of these complexes were then studied. Their emission spectra are depicted in Figure 7, and the positions of the luminescence maxima are summarized in Table 4. Mononuclear ruthenium complex **5** was previously found to exhibit a broad luminescence band at 709 nm with a luminescence quantum yield of 0.057%.[18] The emission of diruthenium complex **13** moves into the NIR region, displaying a broad luminescence band at 793 nm, albeit with a lower quantum yield of 0.023%.[18] This is in accordance with the energy gap law,[28] which states that the nonradiative decay rate increases, and accordingly the quantum yield decreases, as the energy gap or emission gap decreases. It is interesting and gratifying to find that the Ru−Pt complex **7** emits NIR light as well and even with a higher quantum yield (0.15%) than that of the mononuclear ruthenium complex **5**. The position of the emission band (780 nm) is closely similar to that of the diruthenium complex **13**. Considering that

dx.doi.org/10.1021/ic1023696 |*Inorg. Chem.* 2011, 50, 3959–3969

Table 4. Absorption and Emission Data of Complexes Studied[a]

entry	complex	absorption λ_{max}/nm ($\varepsilon/10^5$ $M^{-1}cm^{-1}$)	emission[b] λ_{max}/nm (quantum yield)
1	**5**, $[(bpy)_2Ru(dpdpz)]^{2+}$	299 (0.63), 360 (0.23), 446 (0.10), 490 (0.088)	709 (0.057%)
2	**7**, $[(bpy)_2Ru(dpdpz)PtC{\equiv}CPh]^{2+}$	286 (0.78), 380 (0.30), 436 (0.2) 477 (0.2), 545 (0.2)	780 (0.15%)
3	**8**, $[(bpy)_2Ru(dpdpz)PtC{\equiv}CC_6H_4NMe_2]^{2+}$	288 (0.83), 370 (0.22), 390 (0.22) 478 (0.17), 539 (0.14), 675 (0.09)	
4	**9**, $[(bpy)_2Ru(dpdpz)PtC{\equiv}CC_6H_4Cl]^{2+}$	286 (0.91), 380 (0.26), 432 (0.18) 480 (0.17), 550 (0.15)	784 (0.14%)
5	**13**, $[(bpy)_2Ru(dpdpz)Ru(bpy)_2]^{4+}$	285 (0.87), 360 (0.41), 423 (0.19) 496 (0.22)	793 (0.023%)
6	**10**, $[(tpy)Ru(dpdpz)]^{+}$	276 (0.37), 319 (0.37), 360 (0.20) 427 (0.053), 515 (0.13)	
7	**12**, $[(tpy)Ru(dpdpz)PtC{\equiv}CPh]^{+}$	274 (0.82), 315 (0.65), 372 (0.32) 394 (0.33), 561 (0.40)	
8	**14**, $[(tpy)Ru(dpdpz)Ru(tpy)]^{2+}$	276 (0.71), 316 (0.70), 384 (0.37) 574 (0.48)	
9	$[Ru(bpy)_3](PF_6)_2$	285 (0.65), 354 (0.051) 420 (0.087), 455 (0.11)	612 (5.9%)

[a] All spectra were recorded in a conventional 1.0 cm quartz cell in acetonitrile. [b] The excitation wavelength is 400 nm for all compounds studied. Quantum yield is determined by comparing with a standard sample $[Ru(bpy)_3](PF_6)_2$, which has a quantum yield of 5.9% in N_2-saturated acetonitrile.

Table 5. Excitation Energy (E), Oscillator Strength (f), Dominant Contributing Transitions, and the Associated Percent Contribution and Assignment of Complex 7[a]

S_n	E/eV	E/nm	f	dominant transitions (percent contribution[b])	assignment[c]
1	1.73	716	0.0315	HOMO → LUMO (72%)	M_{Pt}LCT/LLCT
2	1.88	660	0.292	HOMO → LUMO+1 (65%)	M_{Pt}LCT/LLCT
3	2.03	610	0.0545	HOMO-2 → LUMO (34%)	M_{Pt}LCT/ILCT
				HOMO-1 → LUMO (22%)	M_{Pt}LCT
				HOMO-2 → LUMO+1 (12.5%)	M_{Pt}LCT/ILCT
				HOMO-3 → LUMO (11.5%)	M_{Ru}LCT
5	2.12	585	0.0081	HOMO-3 → LUMO (72%)	M_{Ru}LCT
7	2.35	528	0.246	HOMO-2 → LUMO+1 (37%)	M_{Pt}LCT/ILCT
				HOMO-2 → LUMO (18%)	M_{Pt}LCT/ILCT
				HOMO-1 → LUMO+1 (11.5%)	M_{Pt}LCT
				HOMO-1 → LUMO (7.2%)	M_{Pt}LCT
				HOMO-3 → LUMO (5.8%)	M_{Ru}LCT
11	2.46	504	0.0357	HOMO-3 → LUMO+1 (56%)	M_{Ru}LCT
14	2.56	484	0.0667	HOMO-5 → LUMO (37%)	M_{Ru}LCT
				HOMO-3 → LUMO (30%)	M_{Ru}LCT
18	2.77	447	0.0623	HOMO-5 → LUMO+1 (65%)	M_{Ru}LCT
21	2.92	424	0.0344	HOMO-5 → LUMO+2 (39%)	$M_{Ru}L_{bpy}$CT
23	2.95	420	0.213	HOMO-8 → LUMO (58%)	ILCT
28	3.04	408	0.114	HOMO-8 → LUMO+1 (60.5%)	ILCT

[a] Computed at the TDDFT/LANL2DZ level of theory. [b] The actual percent contribution = (configuration coefficient)^2 × 2 × 100%. [c] Otherwise noted, the acceptor of CT transition is dpdpz.

monometallic platinum component emits at a similar energy region as that of $[Ru(bpy)_3]^{2+}$ (around 600 nm),[14,26] it is difficult to determine the nature of the emission of **7**. However, as indicated by TDDFT results, the lowest energy absorption is predominantly attributed to the charge transfer transition from the platinum component. At this stage, we believe that the emission of **7** is of Pt-based MLCT nature mixed with LLCT/ILCT character, as a result of an efficient energy transfer process from the excited Ru-based MLCT state to the Pt-based charge transfer level.[29] This could also explain why the emission quantum yield of **7** is higher than that of **5**. The excitation spectrum of **7** in parallel with its absorption and emission spectra are shown on the right side panel of Figure 7. It confirms that the emission at 780 nm of **7** could be observed by excitation at charge transfer absorption from both metal components, which supports the energy transfer mechanism. Detailed studies of the nature of the emission of **7** and the dynamics of the energy transfer process are currently ongoing. It should also be noted that the emission energy of **7** remains unchanged in the concentration range of 5×10^{-6} to 10^{-4} M (Figure S3 in the Supporting Information). This suggests that no excimer emission could be detected at high concentration. However, the emission intensity decreases when the concentration is increased from 5×10^{-5} to 1×10^{-4} M. This phenomenon is attributed to a self-quenching effect, as is commonly observed in many organometallic complexes including platinum complexes.[25,26,30]

The emission of complex **9** with an electron-withdrawing Cl substituent is slightly more red-shifted than that of **7**, which is in agreement with their absorption spectra. It should be noted that the emission spectra of **7** and **9** are independent of the excitation wavelength, and the quantum yield is around 10% less in air-purged solution. However, we did not detect emission of the dimethylamino-containing complex **8** at room temperature in fluidic solution. The emission from the excited MLCT state is quenched by the low-lying nonemissive LLCT state, as well as by reductive electron transfer from the electron-rich amino group.[27]

dx.doi.org/10.1021/ic1023696 |*Inorg. Chem.* 2011, 50, 3959–3969

Table 6. Excitation Energy (E), Oscillator Strength (f), Dominant Contributing Transitions, and the Associated Percent Contribution and Assignment of Complex 12[a]

S_n	E/eV	E/nm	f	dominant transitions (percent contribution[b])	assignment[c]
2	1.87	664	0.0734	HOMO → LUMO (65%)	$M_{Pt}LCT/LLCT$
				HOMO-1 → LUMO (17%)	$M_{Ru/C}LCT$
4	1.92	644	0.0143	HOMO-1 → LUMO (60.5%)	$M_{Ru/C}LCT$
				HOMO → LUMO (24.5%)	$M_{Pt}LCT/LLCT$
6	2.07	599	0.0235	HOMO-1 → LUMO+2 (72%)	$M_{Ru/C}L_{tpy}CT$
7	2.13	583	0.53	HOMO → LUMO+1 (67%)	$M_{Pt}LCT/LLCT$
				HOMO-1 → LUMO+1 (8.8%)	$M_{Ru/C}LCT$
				HOMO-1 → LUMO (4.5%)	$M_{Ru/C}LCT$
				HOMO-1 → LUMO+2 (4.5%)	$M_{Ru/C}L_{tpy}CT$
8	2.30	540	0.025	HOMO-3 → LUMO (58%)	$M_{Pt}LCT/M_{Ru/C}LCT$
13	2.48	500	0.059	HOMO-2 → LUMO+3 (90%)	$M_{Ru}L_{tpy}CT$
15	2.51	494	0.333	HOMO-5 → LUMO (42%)	$M_{Pt/C}LCT$
				HOMO-3 → LUMO+1 (20%)	$M_{Pt}LCT/M_{Ru/C}LCT$
24	3.00	413	0.106	HOMO-6 → LUMO (70%)	ILCT
27	3.08	403	0.0846	HOMO-6 → LUMO+1 (61%)	ILCT

[a] Computed at the TDDFT/LANL2DZ level of theory. [b] The actual percent contribution = (configuration coefficient)^2 × 2 × 100%. [c] Otherwise noted, the acceptor of CT transition is dpdpz.

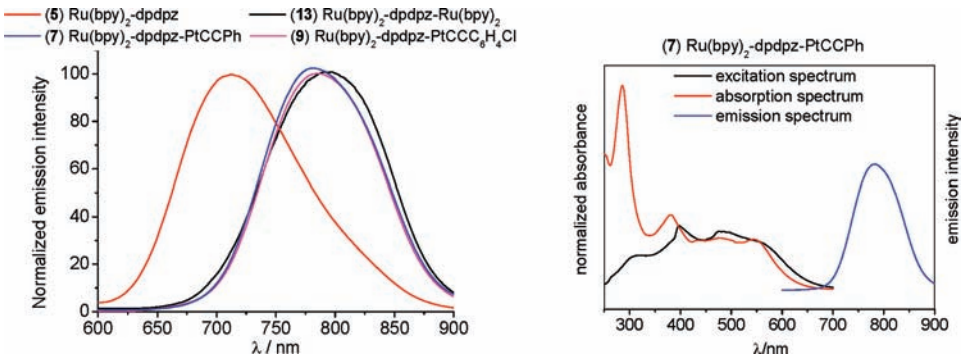

Figure 7. Left: emission spectra of complexes **5**, **7**, **9**, and **13** in acetonitrile. The excitation wavelength is 400 nm. Right: excitation spectrum for emission at 780 nm in parallel with absorption and emission spectra of **7**.

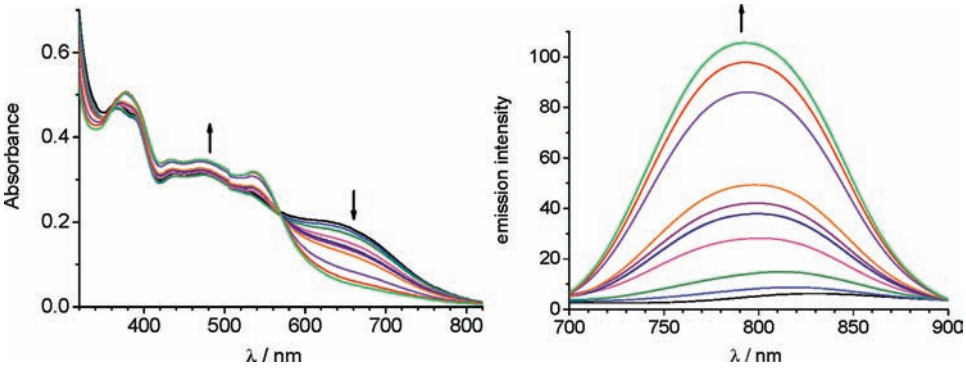

Figure 8. Left: absorption spectral changes of **8** (concentration = 0.020 mM) in acetonitrile with increasing concentrations of *p*-toluenesulfonic acid (from 0 to 0.002, 0.004, 0.006, 0.008, 0.010, 0.014, 0.016, 0.018, and 0.020 mM, respectively). Right: corresponding emission spectral changes of the same solutions with increasing concentrations of *p*-toluenesulfonic acid. The excitation wavelength is 350 nm. The weak band at 820 is probably due to instrumental artifact.

Complex **12** with a cyclometalated ruthenium center was found to give no emission at room temperature either. A possible emissive Pt-based MLCT state could be quenched by the Ru-based moiety. We[18] and others[31] have previously found that the cyclometalated ruthenium moiety could effectively quench the noncyclometalated Ru-based MLCT emissions. However, it might also be possible that the photomultiplier tube R928F we used for the emission measurement is not sufficiently red sensitive to detect any, if indeed present, low-energy weak emission of these complexes.

dx.doi.org/10.1021/ic1023696 |*Inorg. Chem.* 2011, 50, 3959–3969

The spectroscopic properties of the dimethylamine-containing complex **8** were further studied by acidic titration experiment. Upon gradual addition of *p*-toluenesulfonic acid, solutions of **8** in acetonitrile exhibit remarkable color changes from brownish green to red (Figure S4 in the Supporting Information). Accordingly, the electronic absorption spectra displayed a significant decrease of the LLCT band (580−800 nm) and slight enhancement of the MLCT bands (400−560 nm, left in Figure 8). This is result of the protonation of the NMe_2 group by *p*-toluenesulfonic acid. The formation of a well-defined isosbestic point at 568 nm indicates a clean protonation process. As shown in the right panel of Figure 8, the emission intensity of **8** was greatly enhanced with increasing concentration of *p*-toluenesulfonic acid. The revival of emission is a result of the disappearance of the reductive electron transfer quenching pathway upon protonation of the amino group.[27] The emission maximum is around 790 nm, which is similar to those of complexes **7**, **9**, and **13**. The reversibility of the protonation process was demonstrated by the recovery of the LLCT absorption band and the decrease of emission intensity upon further addition of 1 equiv of triethylamine to the protonated **8** (Figures S5 and S6 in the Supporting Information).

CONCLUSIONS

To summarize, the reaction of dpdpz with K_2PtCl_4 afforded mono-Pt complex **4** with two lateral pyridine nitrogen atoms binding to the metal center, as is proved by its X-ray single crystal structure. Cyclometalated platinum complexes based on dpdpz could be prepared starting from mono-Ru complex **5** or **10**. In this way, two types of $Ru^{II}-Pt^{II}$ heterodimetallic complexes bridged by dpdpz, namely, $[(bpy)_2Ru(dpdpz)Pt(C{\equiv}CC_6H_4R)]^{2+}$ and $[(tpy)Ru(dpdpz)Pt(C{\equiv}CPh)]^{+}$, were produced. The electronic properties of these complexes could be modulated by the coordination mode of ruthenium atom with dpdpz (N^N bidentate or C^N^N tridentate). These complexes exhibit substantial absorption in the visible to NIR region because of mixed LLCT, ILCT, and MLCT transitions from both metal centers. This would make them good light-harvesting materials. Complex $[(bpy)_2Ru(dpdpz)Pt(C{\equiv}CPh)]^{2+}$ (**7**) was found to emit NIR light (centered at 780 nm) with higher quantum yield than that of the mono-Ru complex $[(bpy)_2Ru(dpdpz)]^{2+}$ (**5**). This could be a result of efficient energy transfer from the $Ru(bpy)_2$ moiety to the platinum component. No emission was detected from $[(tpy)Ru(dpdpz)Pt(C{\equiv}CPh)]^{+}$, which could be attributable to a reversed energy transfer process from the platinum moiety to the Ru(tpy) component, and the work on the dynamics of these processes is currently on the way. The NMe_2-containing complex **8** was found to display remarkable color changes and emit NIR light upon gradual protonation, and this fact could be used for colorimetric and luminescence pH sensors.[27] The attachment of the Pt(C^N^N) moiety to mono-Ru complex **5** or **10** induces significant changes of the electrochemical properties as well. Particularly important is that the first reduction of the bridging ligand was found to occur at a much less negative potential, and this effect is stronger than the case when a cyclometalated Ru(tpy) moiety is coordinated to **5** or **10**. The work described in this article illustrated the capability of dpdpz as a bridging ligand for the synthesis of heterodinuclear coordination compounds. Future studies will focus on the design and synthesis of new transitional metal complexes bridged by dpdpz, with the aim of improving the emission qualities of these NIR emitting materials.

EXPERIMENTAL SECTION

Computational Method. Rough geometries of **7** and **12** were generated using the MOPAC 09 software package and the semiempirical PM6 method, which includes parametrization for 70 elements.[32] Resulting geometries were then relaxed without constraints using Gaussian03 at the DFT level.[33,34] Structure optimizations were performed using the B3LYP hybrid functional.[35] The B3LYP hybrid functional was used based on good agreement for enthalpies of formation,[36] ionization potentials and electron affinities,[37] and band gaps[38] with experimental data. No symmetry constraints were used in the optimization (SCF = NoSymm keyword); the initial symmetry was set to C_1. Wave functions were expanded in the LANL2DZ basis set with effective core potentials.[39] Solvation effects in acetonitrile were included using the conductor-like polarizable continuum model (CPCM) with united-atom Kohn−Sham (UAKS) radii.[40] Previous studies have shown that this method is effective for calculating solvation energies for cations in aqueous environments.[41] The extension to other polar solvents is not unreasonable.

Spectroscopic Measurements. All optical ultraviolet−visible (UV/vis) absorption spectra were obtained using a TU-1810DSPC spectrometer of Beijing Purkinje General Instrument Co. Ltd. at room temperature in acetonitrile, with a conventional 1 cm quartz cell. Emission spectra were recorded using a F-380 spectrofluorimeter of Tianjin Gangdong Sic & Tech Development Co. Ltd., with a red-sensitive photomultiplier tube R928F. Samples for emission measurement were obtained within quartz cuvettes of 1 cm path length. Luminescence quantum yields were determined using $[Ru(bpy)_3](PF_6)_2$ in degassed acetonitrile solution as the standard (ϕ = 5.9%);[42] estimated uncertainty of ϕ is ±10% or better.

Electrochemical Measurements. All cyclic voltammetry (CV) measurements were taken using a CHI620D potentiostat with one-compartment electrochemical cell under an atmosphere of nitrogen. A glassy carbon electrode with a diameter of 0.3 mm was used as the working electrode. The electrode was polished prior to use with 0.05 μm alumina and rinsed thoroughly with water and acetone. A large area platinum wire coil was used as the counter electrode. All potentials are referenced to a saturated Ag/AgCl electrode without regard for the liquid junction potential. All measurements were carried out in acetonitrile at a scan rate of 100 mV/s, in 0.1 M of Bu_4NClO_4 (TBAP) as the supporting electrolyte.

Synthesis. All reactions were carried out under an atmosphere of dry nitrogen using standard Schlenk techniques. Dry tetrahydrofuran was distilled from sodium/benzophenone, and other solvents (analytical grade) were used without further purification. NMR spectra were recorded in the designated solvent on a Varian 300 or Bruker Avance 400 M spectrometer. MS data were obtained with a Bruker Daltonics Inc. ApexII FT-ICR or Autoflex III MALDI-TOF mass spectrometer. The matrix for MALDI-TOF measurement is 2,5-dihydroxybenzoic acid (DHB) or α-cyano-4-hydroxycinnamic acid (CCA). Microanalysis was carried out using Flash EA 1112 or Carlo Erba 1106 analyzer at the Institute of Chemistry, CAS.

$PtCl_2$-dpdpz (4). A suspension of the dpdpz ligand **1** (77 mg, 0.2 mmol) and potassium tetrachloroplatinate (170 mg, 0.41 mmol) in CH_3CN/H_2O (10 mL/10 mL) was refluxed under N_2 for 24 h. After cooling, the precipitate was collected after filtration and washed with water and ether to give the product (120 mg, 90% yield). ^1H NMR (300 MHz, $CDCl_3$): δ 7.35−7.50 (m, 8H), 7.62 (d, J = 7.8 Hz, 4H), 7.86−7.98 (m, 4H), 9.22 (d, J = 5.7 Hz, 2H). TOF-ESI, 653 for $[M+H]^+$, 617 for $[M + H - Cl]^+$. ESI-HRMS calcd. 653.0636 for $[M+H]^+$ ($C_{26}H_{19}N_4Cl_2Pt$), found 653.0641. Anal. Calcd. for $C_{26}H_{18}Cl_2N_4Pt$: C, 47.86; H, 2.78; N, 8.59. Found: C, 47.68; H, 2.54; N, 8.39.

$[(bpy)_2Ru$-dpdpz-PtCl$](PF_6)_2$ (6). To a solution of Ru^{II} monomer **5** (54 mg, 0.05 mmol) in 8 mL of acetonitrile were added 8 mL of

aqueous solution of K_2PtCl_4 (41 mg, 0.1 mmol). The mixture was refluxed for 24 h under a nitrogen atmosphere. The organic solvent was evaporated before adding an excess of KPF_6 and water. The resulting precipitates were collected to afford 54 mg of deep red solid **5** in a yield of 82%. This crude product was used for the next transformation without further purification. MALDI-MS: 1173.3 for $[M - H - PF_6]^+$, 1026.3 for $[M - 2H - 2PF_6]^{2+}$.

[(bpy)$_2$Ru-dpdpz-Pt-≡-Ph](PF$_6$)$_2$ (7). To a mixture of nitrogen saturated DMF (10 mL) and triethylamine (2 mL) were added the above-prepared complex **6** (52 mg, 0.04 mmol), CuI (4 mg), and phenylacetylene (0.3 mL). The mixture was stirred in a dark at room temperature for 28 h. After removing the organic solvent by distillation under vacuum, the residue was subject to flash column chromatography on silica gel to afford 27 mg of **7** (54% yield). MALDI-MS: 1240.4 for $[M - PF_6]^+$, 1095.5 for $[M + H - 2PF_6]^{2+}$, 938.5 for $[M - bpy - 2PF_6]^{2+}$. IR (KBr, cm^{-1}): 3426, 3050, 2920, 2100 ($\nu_{C\equiv C}$), 1569, 1444, 1397, 1165, 840, 761, 559. Anal. Calcd. for $C_{54}H_{38}F_{12}N_8P_2RuPt$: C, 46.83; H, 2.77; N, 8.09. Found: C, 46.42; H, 2.85; N, 8.02.

[(bpy)$_2$Ru-dpdpz-Pt-≡-C$_6$H$_4$NMe$_2$](PF$_6$)$_2$ (8). To a mixture of nitrogen saturated dimethylformamide (DMF, 10 mL) and triethylamine (2 mL) were added complex **6** (65 mg,0.05 mmol), CuI (4 mg), and 1-*N*,*N*-dimethylamino-4-ethynylbenzene (14 mg, 0.09 mmol). The mixture was stirred in the dark at room temperature for 24 h. After removing the organic solvent by distillation under vacuum, the residue was subject to flash column chromatography on silica gel to afford 20 mg of **8** (28% yield). MALDI-MS: 1138.5 for $[M - 2PF_6]^{2+}$, 981.5 for $[M - bpy - 2PF_6]^{2+}$. IR (KBr, cm^{-1}): 3415, 3078, 2930, 2097 ($\nu_{C\equiv C}$), 1719, 1603, 1445, 1290, 1126, 843, 763, 559. Anal. Calcd. for $C_{56}H_{43}F_{12}N_9P_2RuPt\cdot H_2O$: C, 46.51; H, 3.14; N, 8.72. Found:C, 46.24; H, 3.32; N, 8.89.

[(bpy)$_2$Ru-dpdpz-Pt-≡-C$_6$H$_4$Cl](PF$_6$)$_2$ (9). To a mixture of nitrogen saturated DMF (10 mL) and triethylamine (2 mL) were added complex **6** (62 mg, 0.047 mmol), CuI (4 mg), and 1-chloro-4-ethynylbenzene (10.8 mg, 0.08 mmol). The mixture was stirred in the dark at room temperature for 18 h. After removing the organic solvent by distillation under vacuum, the residue was subject to flash column chromatography on silica gel to afford 36 mg of **9** (53% yield). MALDI-MS: 974.1 for $[M - bpy - 2PF_6 + H]^{2+}$. IR (KBr, cm^{-1}): 3427, 3081, 2924, 2101 ($\nu_{C\equiv C}$), 1602, 1445, 1397, 1165, 836, 762, 559. Anal. Calcd. for $C_{54}H_{37}ClF_{12}N_8P_2RuPt\cdot H_2O$: C, 45.12; H, 2.73; N, 7.80. Found:C, 44.63; H, 2.62; N, 8.25.

[(tpy)Ru-dpdpz-Pt-Cl](PF$_6$) (11). To a solution of Ru^{II} monomer **10** (43 mg, 0.05 mmol) in 8 mL of acetonitrile were added 8 mL of aqueous solution of K_2PtCl_4 (41 mg, 0.1 mmol). The mixture was refluxed for 20 h under a nitrogen atmosphere. The organic solvent was evaporated before adding an excess of NH_4PF_6. The resulting precipitates were separated and purified by recrystallization in a mixture of acetonitrile and ether (40 mg, 74% yield). This crude product was used for next transformation without further purification. Attempts to purify the product through flash column chromatography led to decomposition. ^{1}H NMR (300 MHz, CD_3CN): δ 5.73 (d, J = 7.2 Hz, 1H), 6.74 (t, J = 7.2 Hz, 1H), 7.16 (m, 2H), 7.42 (d, J = 5.1 Hz, 1H), 7.50−7.70 (m, 7H), 7.80 (t, J = 7.2 Hz, 1H), 7.98 (m, 2H), 8.04−8.30 (m, 4H), 8.32−8.62 (m, 7H), 9.14 (d, J = 5.1 Hz, 1H). ESI-MS 949.9 for $[M - PF_6]^+$.

[(tpy)Ru-dpdpz-Pt-≡-Ph](PF$_6$) (12). To a mixture of nitrogen saturated DMF (5 mL) and triethylamine (1 mL) were added Ru−Pt complex **11** (27 mg), CuI (2 mg), and phenylacetylene (0.1 mL). The mixture was stirred in the dark at room temperature for 48 h. After removing the organic solvent by distillation under vacuum, the residue was subject to flash column chromatography on silica gel to afford 15 mg of **12** (54% yield). ^{1}H NMR (300 MHz, CD_3CN): δ 5.73 (d, J = 7.5 Hz, 1H), 6.74 (m, 2H), 7.10 (m, 3H), 7.20−7.41 (m, 6H), 7.58 (m, 4H), 7.69 (d, J = 5.1 Hz, 1H), 7.82 (m, 4H), 8.07−8.27 (m, 4H), 8.38−8.68 (m, 3H), 8.64 (d, J = 8.1 Hz, 1H), 8.70 (d, J = 8.1 Hz, 2H), 9.18 (d, J = 5.4 Hz, 1H). IR (KBr, cm^{-1}): 3437, 3056, 2928, 2103 ($\nu_{C\equiv C}$), 1598, 1446, 1283, 1020, 843, 764, 559. ESI-MS 1014.1 for $[M - PF_6]^+$. ESI-HRMS calcd. 1014.1423 for $[M - PF_6]^+$ ($C_{49}H_{32}N_7RuPt$), found 1014.1424.

■ ASSOCIATED CONTENT

Supporting Information. CV profiles of **8** and **9**, emission spectra of **7** at different concentrations, absorption and emission spectral changes of protonated **8** upon addition of triethylamine, complete reference,[32] and the crystallographic data of **4** in CIF format. This material is available free of charge via the Internet at http://pubs.acs.org.

■ AUTHOR INFORMATION

Corresponding Author

*E-mail: zhongyuwu@iccas.ac.cn (Y.-W.Z.), hda1@cornell.edu (H.D.A.).

■ ACKNOWLEDGMENT

We thank the National Natural Science Foundation of China (Grant 21002104), 973 program (Grant 2011CB932300), and the Institute of Chemistry, Chinese Academy of Sciences ("100 Talent" Program) for funding support. This work was also supported by the Center for Molecular Interfacing, an NSF Phase I Center for Chemical Innovation award (0847926) and the Cornell Center for Materials Research (CCMR). Some DFT calculations were performed on the Intel Cluster at the Cornell Nanoscale Facility, part of the National Nanotechnology Infrastructure Network (NNIN) funded by the National Science Foundation (NSF).

■ REFERENCES

(1) (a) Fabian, J.; Makazumi, H.; Matsuoka, M. *Chem. Rev.* **1992**, *92*, 1197. (b) Qian, G.; Wang, Z. Y. *Chem. Asian J.* **2010**, *5*, 1006.

(2) (a) Mayerhöffer, U.; Deing, K.; Gruβ, K.; Braunschweig, H.; Meerholz, K.; Würthner, F. *Angew. Chem., Int. Ed.* **2009**, *48*, 8776. (b) Mor, G. K.; Kim, S.; Paulose, M.; Varghese, O. K.; Shankar, K.; Basham, J.; Grimes, C. A. *Nano Lett.* **2009**, *9*, 4250. (c) Hyun, B.-R.; Zhong, Y.-W.; Bartnik, A. C.; Sun, L.; Abruña, H. D.; Wise, F. A.; Goodreau, J. D.; Mattews, J. R.; Leslie, T. M.; Borrelli, N. F. *ACS Nano* **2008**, *2*, 2206.

(3) (a) Qian, G.; Zhong, Z.; Luo, M.; Yu, D.; Zhang, Z.; Yang, Z. Y.; Ma, D. *Adv. Mater.* **2009**, *21*, 111. (b) Godbert, N.; Dattilo, D.; Termine, R.; Aiello, I.; Bellusci, A.; Crispini, A.; Golemme, A.; Ghedini, M. *Chem. Asian J.* **2009**, *4*, 1141.

(4) (a) McDonnell, S. O.; O'Shea, D. F. *Org. Lett.* **2006**, *8*, 3493. (b) Ran, C.; Xu, X.; Raymond, S. B.; Ferrara, B. J.; Neal, K.; Bacskai, B. J.; Medarova, Z.; Moore, A. *J. Am. Chem. Soc.* **2009**, *131*, 15267. (c) Kiyose, K.; Kojima, H.; Urano, Y.; Nagano, T. *J. Am. Chem. Soc.* **2006**, *128*, 6548.

(5) (a) Umezawa, K.; Nakamura, Y.; Makino, H.; Citterio, D.; Suzuki, K. *J. Am. Chem. Soc.* **2008**, *130*, 1550. (b) Loudet, A.; Bandichhor, R.; Burgess, K.; Palma, A.; McDonnell, S. O.; Hall, M. J.; O'Shea, D. F. *Org. Lett.* **2008**, *10*, 4771.

(6) (a) Xie, R.; Peng, X. *J. Am. Chem. Soc.* **2009**, *131*, 10645. (b) Blackman, B.; Battaglia, D.; Peng, X. *Chem. Mater.* **2008**, *20*, 4847. (c) Du, Y.; Xu, B.; Fu, T.; Cai, M.; Li, F.; Zhang, Y.; Wang, Q. *J. Am. Chem. Soc.* **2010**, *132*, 1470.

(7) (a) Jiao, C.; Huang, K.-W.; Luo, J.; Zhang, K.; Chi, C.; Wu, J. *Org. Lett.* **2009**, *11*, 4508. (b) Pschirer, N. G.; Kohl, C.; Nolde, F.; Qu, J.; Müllen, K. *Angew. Chem., Int. Ed.* **2006**, *45*, 1401.

(8) (a) Ward, M. D.; McCleverty, J. A. *J. Chem. Soc., Dalton Trans.* **2002**, 275. (b) Chen, J.-L.; Chi, Y.; Chen, K.; Cheng, Y.-M.; Chung, M.-W.;

Yu, Y.-C.; Lee, G.-H.; Chou, P.-T.; Shu, C.-F. *Inorg. Chem.* **2010**, *49*, 823. (c) Treadway, J. A.; Strouse, G. F.; Ruminski, R. R.; Meyer, T. J. *Inorg. Chem.* **2001**, *40*, 4508.

(9) (a) Schubert, U. S.; Eschbaumer, C. *Angew. Chem., Int. Ed.* **2002**, *41*, 2892. (b) Harriman, A.; Ziessel, R. *Chem. Commun.* **1996**, 1707. (c) Balzani, V.; Juris, A.; Venturi, M. *Chem. Rev.* **1996**, *96*, 759. (d) Barigelletti, F.; Flamigni, L. *Chem. Soc. Rev.* **2000**, *29*, 1. (e) Ziessel, R. *Synthesis* **1999**, 1839. (f) Balzani, V.; Juris, A. *Coord. Chem. Rev.* **2001**, *211*, 97. (g) Eryazici, I.; Moorefield, C. N.; Newkome, G. R. *Chem. Rev.* **2008**, *108*, 1834. (h) Constable, E. C. *Chem. Soc. Rev.* **2007**, *36*, 246. (i) Medlycott, E. A.; Hanan, G. S. *Chem. Soc. Rev.* **2005**, *34*, 133. (j) Baranoff, E.; Collin, J.-P.; Flamigni, L.; Sauvage, J.-P. *Chem. Soc. Rev.* **2004**, *33*, 147.

(10) (a) Arana, C. R.; Abruña, H. D. *Inorg. Chem.* **1993**, *32*, 194. (b) Chanda, N.; Sarkar, B.; Kar, S.; Fiedler, J.; Kaim, W.; Lahiri, G. K. *Inorg. Chem.* **2004**, *43*, 5128. (c) Hartshom, C. M.; Daire, N.; Tondreau, V.; Loeb, B.; Meyer, T. J.; White, P. S. *Inorg. Chem.* **1999**, *38*, 3200. (d) Dattelbaum, D. M.; Hartshom, C. M.; Meyer, T. J. *J. Am. Chem. Soc.* **2002**, *124*, 4938.

(11) (a) Balzani, V.; Campagna, S.; Denti, G.; Juris, A.; Serroni, S.; Venturi, M. *Acc. Chem. Res.* **1998**, *31*, 26. (b) Serroni, S.; Juris, A.; Campagna, S.; Venturi, M.; Denti, G.; Balzani, V. *J. Am. Chem. Soc.* **1994**, *116*, 9086. (c) D'Alessandro, D. M.; Dinolfo, P. H.; Davis, M. S.; Hupp, J. T.; Keene, F. R. *Inorg. Chem.* **2006**, *45*, 3261. (d) Milkevitch, M.; Brauns, E.; Brewer, K. J. *Inorg. Chem.* **1996**, *35*, 1737. (e) Marcaccio, M.; Paolucci, F.; Paradisi, C.; Roffia, S.; Fontanesi, C.; Yellowlees, L. J.; Serroni, S.; Campagna, S.; Denti, G.; Balzani, V. *J. Am. Chem. Soc.* **1999**, *121*, 10081.

(12) (a) Albrecht, M. *Chem. Rev.* **2010**, *110*, 576. (b) Bruce, M. I. *Angew. Chem., Int. Ed. Engl.* **1977**, *16*, 73.

(13) (a) Ulbricht, C.; Beyer, B.; Friebe, C.; Winter, A.; Schubert, U. S. *Adv. Mater.* **2009**, *21*, 4418. (b) You, Y.; Park, S. Y. *Dalton Trans.* **2009**, 1267.

(14) (a) Lu, W.; Mi, B.-X.; Chan, M. C. W.; Hui, Z.; Che, C.-M.; Zhu, N.; Lee, S.-T. *J. Am. Chem. Soc.* **2004**, *126*, 4958. (b) Shao, P.; Li, Y.; Yi, J.; Pritchett, T. M.; Sun, W. *Inorg. Chem.* **2010**, *49*, 4507. (c) Hofmann, A.; Dahlenburg, L.; van Eldik, R. *Inorg. Chem.* **2003**, *42*, 6528.

(15) (a) Djukic, J.-P.; Sortais, J.-B.; Barloy, L.; Pfeffer, M. *Eur. J. Inorg. Chem.* **2009**, 817. (b) Jäger, M.; Smeigh, A.; Lombeck, F.; Görls, H.; Collin, J.-P.; Sauvage, J.-P.; Hammarström, L.; Johansson, O. *Inorg. Chem.* **2010**, *49*, 374. (c) Wadman, S. H.; Lutz, M.; Tooke, D. M.; Spek, A. L.; Hartl, F.; Havenith, R. W. A.; van Klink, G. P. M.; van Koten, G. *Inorg. Chem.* **2009**, *48*, 1887. (d) Wadman, S. H.; Havenith, R. W. A.; Hartl, F.; Lutz, M.; Spek, A. L.; van Klink, G. P. M.; van Koten, G. *Inorg. Chem.* **2009**, *48*, 5685. (e) Bomben, P. G.; Robson, K. C. D.; Sedach, P. A.; Berlinguette, C. P. *Inorg. Chem.* **2009**, *48*, 9631. (f) Bomben, P. G.; Koivisto, B. D.; Berlinguette, C. P. *Inorg. Chem.* **2010**, *49*, 4960. (g) Yao, C.-J.; Sui, L.-Z.; Xie, H.-Y.; Xiao, W.-J.; Zhong, Y.-W.; Yao, J. *Inorg. Chem.* **2010**, *49*, 8347. (h) Vilà, N.; Zhong, Y.-W.; Henderson, J. C.; Abruña, H. D. *Inorg. Chem.* **2010**, *49*, 796.

(16) Williams, J. A. G.; Beeby, A.; Davis, E. S.; Weinstein, J. A.; Wilson, C. *Inorg. Chem.* **2003**, *42*, 8609.

(17) Cheung, T.-C.; Cheung, K.-K.; Peng, S.-M.; Che, C.-M. *J. Chem. Soc., Dalton Trans.* **1996**, 1645.

(18) Zhong, Y.-W.; Wu, S.-H.; Burkhardt, S. E.; Yao, C.-J.; Abruña, H. D. *Inorg. Chem.* **2011**, *50*, 517.

(19) (a) Cárdenas, D. J.; Echavarren, A. M. *Organometallics* **1999**, *18*, 3337. (b) Cave, G. W. C.; Alcock, N. W.; Rourke, J. P. *Organometallics* **1998**, *17*, 1801.

(20) Constable, E. C.; Henney, P. G.; Leese, T. A.; Tocher, D. A. *J. Chem. Soc., Dalton Trans.* **1990**, 443.

(21) (a) Teles, W. M.; Speziali, N. L.; Filgueiras, C. A. L. *Polyhedron* **2000**, *19*, 739. (b) Bitzer, R. S.; San Gil, R. A. S.; Filgueiras, C. A. L. *J. Braz. Chem. Soc.* **2006**, *17*, 1600. (c) Kukushkin, Y. N.; Kiseleva, N. P.; Zangrando, E.; Kukushkin, V. Y. *Inorg. Chim. Acta* **1999**, *285*, 203.

(22) (a) Periana, R. A.; Taube, D. J.; Gamble, S.; Taube, H.; Satoh, T.; Fujii, H. *Science* **1998**, *280*, 560. (b) Lersch, M.; Tilset, M. *Chem. Rev.* **2005**, *105*, 2471.

(23) (a) Toma, L. M.; Armentano, D.; Munno, G. D.; Sletten, J.; Lloret, F.; Julve, M. *Polyhedron* **2007**, *26*, 5263. (b) Carranza, J.; Sletten, J.; Brennan, C.; Lloret, F.; Cano, J.; Julve, M. *Dalton Trans.* **2004**, 3997.

(24) (a) Ji, Y.; Zhang, R.; Li, Y.-J.; Li, Y.-Z.; Zuo, J.-L.; You, X.-Z. *Inorg. Chem.* **2007**, *46*, 866. (b) Hua, F.; Kinayyigit, S.; Rachford, A. A.; Shikhova, E. A.; Goeb, S.; Cable, J. R.; Adams, C. J.; Kirschbaum, K.; Pinkerton, A. A.; Castellano, F. N. *Inorg. Chem.* **2007**, *46*, 8771. (c) Ventura, B.; Barbieri, A.; Barigelletti, F.; Seneclauze, J. B.; Retailleau, P.; Ziessel, R. *Inorg. Chem.* **2008**, *47*, 7048.

(25) (a) James, S. L.; Younus, M.; Raithby, P. R.; Lewis, J. *J. Organomet. Chem.* **1997**, *543*, 233. (b) Hissler, M.; McGarrah, J. E.; Connick, W. B.; Geiger, D. K.; Cummings, S. D.; Eisenberg, R. *Coord. Chem. Rev.* **2000**, *208*, 115. (c) Hissler, M.; Connick, W. B.; Geiger, D. K.; McGarrah, J. E.; Lipa, D.; Lachicotte, R. J.; Eisenberg, R. *Inorg. Chem.* **2000**, *39*, 447. (d) Yam, V. W.-W.; Chan, K. H.-Y.; Wong, K. M.-C.; Chu, B. W.-K. *Angew. Chem., Int. Ed.* **2006**, *45*, 6169. (e) Seneclauze, J. B.; Retailleau, P.; Ziessel, R. *New J. Chem.* **2007**, *31*, 1412.

(26) (a) Cheung, T.-C.; Cheung, K.-K.; Peng, S.-M.; Che, C.-M. *J. Chem. Soc., Dalton Trans.* **1996**, 1645. (b) Yam, V. W.-W.; Tang, R. P.-L.; Wong, K. M.-C.; Cheung, K.-K. *Organometallics* **2001**, *20*, 4476. (c) Lu, W.; Mi, B.-X.; Chan, M. C. W.; Hui, Z.; Zhu, N.; Lee, S.-T.; Che, C.-M. *Chem. Commun.* **2002**, 206. (d) Schneider, J.; Du, P.; Jarosz, P.; Lazarides, T.; Wang, X.; Brennessel, W. W.; Eisenberg, R. *Inorg. Chem.* **2009**, *48*, 4306.

(27) (a) Wong, K. M.; Tang, W.-S.; Lu, X.-X.; Zhu, N.; Yam, V. W.-W. *Inorg. Chem.* **2005**, *44*, 1492. (b) Han, X.; Wu, L.-Z.; Si, G.; Pan, J.; Yang, Q.-Z.; Zhang, L.-P.; Tung, C.-H. *Chem.—Eur. J.* **2007**, *13*, 1231. (c) Ji, Z.; Li, Y.; Sun, W. *J. Organomet. Chem.* **2009**, *694*, 4140.

(28) Freed, K. F. *Acc. Chem. Res.* **1978**, *11*, 74, and references therein.

(29) (a) Juris, A.; Balzani, V.; Campagna, S.; Denti, G.; Serroni, S.; Frei, G.; Güdel, H. U. *Inorg. Chem.* **1994**, *33*, 1491. (b) Puntoriero, F.; Serroni, S.; Licciardello, A.; Venturi, M.; Juris, A.; Ricevuto, V.; Campagna, S. *J. Chem. Soc., Dalton Trans.* **2001**, 1035. (c) Easun, T. L.; Alsindi, W. Z.; Towrie, M.; Ronayne, K. L.; Sun, X.-Z.; Ward, M. D.; George, M. W. *Inorg. Chem.* **2008**, *47*, 5071. (d) Fan, Y.; Zhang, L.-Y.; Dai, F.-R.; Shi, L.-X.; Chen, Z.-N. *Inorg. Chem.* **2008**, *47*, 2811.

(30) Lai, S. W.; Chan, M. C. W.; Cheung, T. C.; Peng, S. M.; Che, C. M. *Inorg. Chem.* **1999**, *38*, 4046.

(31) Ott, S.; Borgström, M.; Hammarström, L.; Johansson, O. *Dalton Trans.* **2006**, 1434.

(32) Stewart, J. J. P. *J. Mol. Model.* **2007**, *13*, 1173.

(33) Frisch, M. J.; et al. *Gaussian 03*, revision E.01; Gaussian, Inc.: Wallingford, CT, 2004. See the Supporting Information for the full list of the authors.

(34) Kohn, W.; Sham, L. *Phys. Rev. A* **1964**, *140*, 1133.

(35) (a) Becke, A. D. *J. Chem. Phys.* **1993**, *98*, 5648. (b) Lee, C.; Yang, W.; Parr, R. G. *Phys. Rev. B* **1988**, *37*, 785.

(36) Curtiss, L. A.; Raghavachari, k.; Redfern, P. C.; Pople, J. A. *Chem. Phys. Lett.* **1997**, *270*, 419.

(37) Zhan, C. G.; Nichols, J. A.; Dixon, D. A. *J. Phys. Chem. A* **2003**, *107*, 4184.

(38) Muscat, J.; Wander, A.; Harrison, N. M. *Chem. Phys. Lett.* **2001**, *342*, 397.

(39) (a) Dunning, T. H.; Hay, P. J. In *Modern Theoretical Chemistry*; Schaefer, H. F., Ed.; Plenum: New York, 1976; Vol. 3, p 1. (b) Hay, P. J.; Wadt, W. R. *J. Chem. Phys.* **1985**, *82*, 270. (c) Wadt, W. R.; Hay, P. J. *J. Chem. Phys.* **1985**, *82*, 284. (d) Hay, P. J.; Wadt, W. R. *J. Chem. Phys.* **1985**, *82*, 299.

(40) (a) Klamt, A.; Schüürmann, G. *J. Chem. Soc., Perkin Trans. 2* **1993**, 799. (b) Andzelm, J.; Kölmel, C.; Klamt, A. *J. Chem. Phys.* **1995**, *103*, 9312. (c) Barone, V.; Cossi, M. *J. Phys. Chem. A* **1998**, *102*, 1995. (d) Cossi, M.; Rega, N.; Scalmani, G.; Barone, V. *J. Comput. Chem.* **2003**, *24*, 669.

(41) Takano, Y.; Houk, K. N. *J. Chem. Theory Comput.* **2005**, *1*, 70.

(42) Nakamura, K. *Bull. Chem. Soc. Jpn.* **1982**, *55*, 1639.